Ultrafine Porous Intermetallic Compounds Fabricated by High-Temperature Liquid Metal Dealloying for Electrochemical Hydrogen Production

○ **Ruirui Song**, Jiuhui Han, Masayuki Okugawa, Rodion Belosludov, Takeshi Wada, Jing Jiang, Daixiu Wei, Akira Kudo, Yuan Tian, Mingwei Chen, Hidemi Kato

東北大学金属材料研究所 加藤研究室

先端エネルギー材料理工共創研究センター(E-IMR)

複合モジュール・社会実装研究ユニット/特任助教

Dec. 22, 2022

Research Background

Sustainable energy future

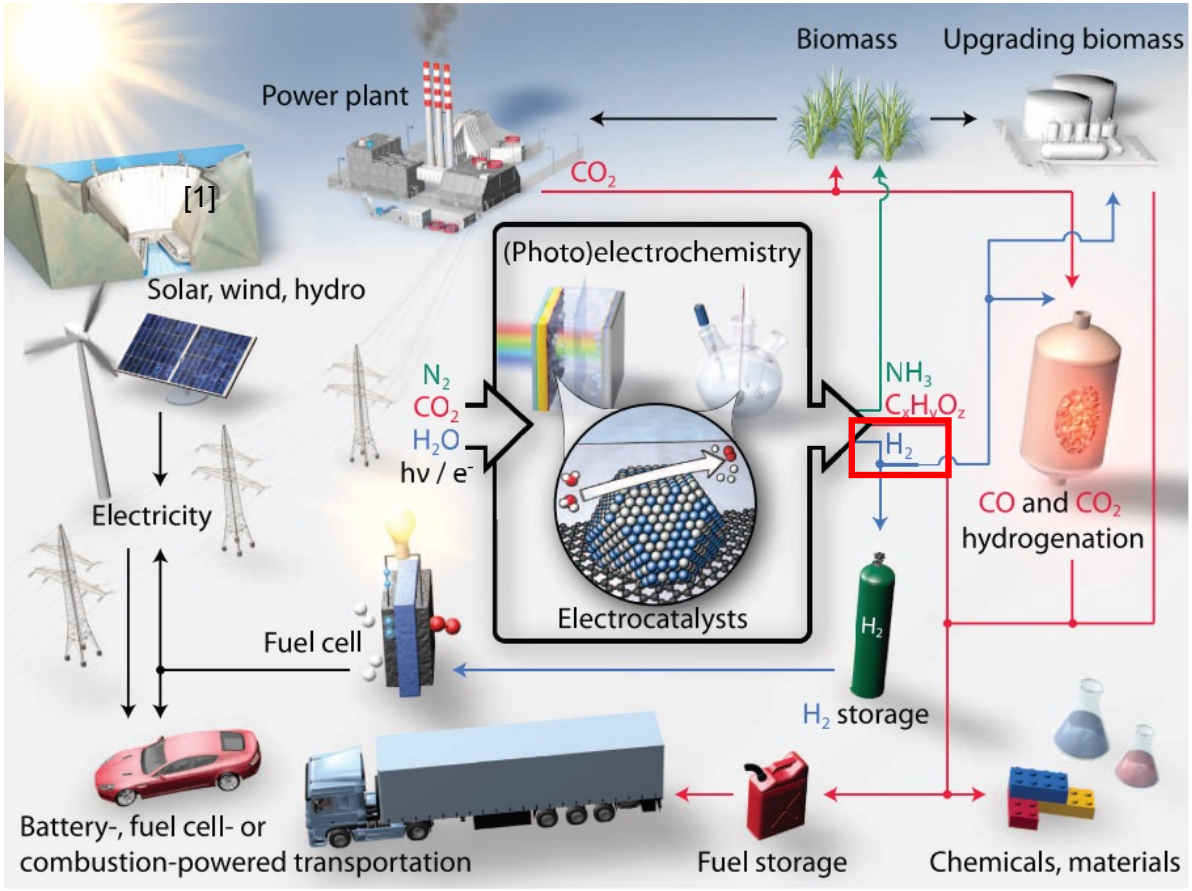

[1] *Science*, *355*(6321), eaad4998.

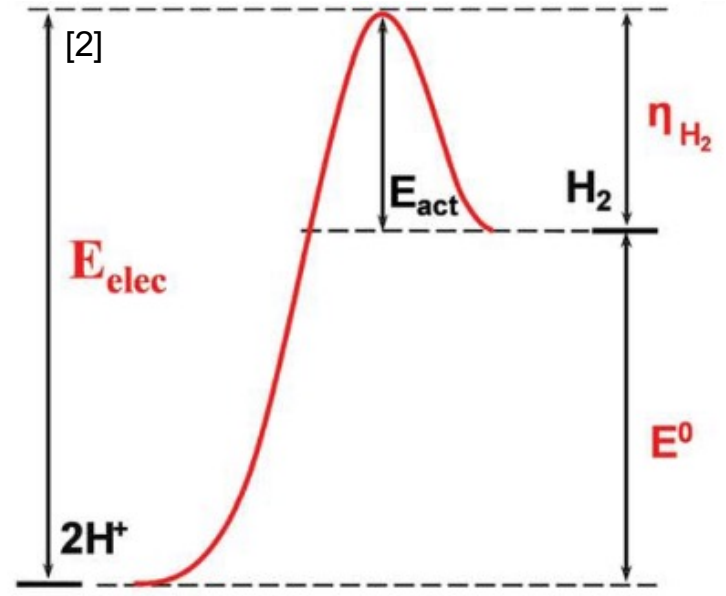

[2] *Journal of Materials Chemistry A* 3.29 (2015): 14942-14962.

Energy barrier

$$H_2O,\ CO_2 \text{ and } N_2 \xrightarrow[\textbf{Electrocatalysts}]{\text{Electrochemical process}} \text{Fuels and Chemicals}$$

How to develop electrocatalysts ?

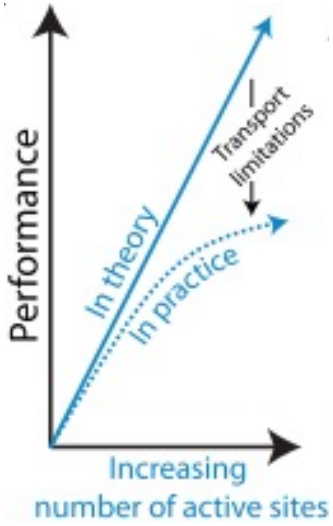

Nanostructuring

Supports

Shape

…

Self-supported 3D bicontinuous open porosity

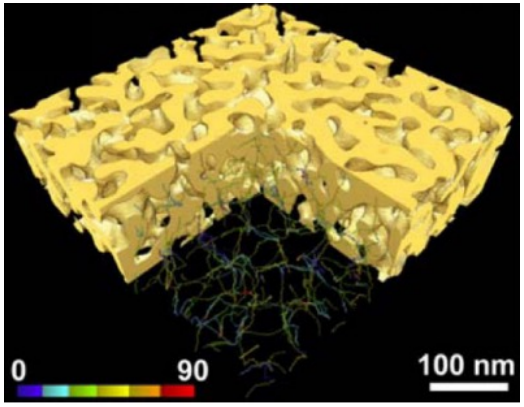

- Large surface area
- Efficient mass transport
- Good electrical conductivity
- Thermal stability

Physical review letters 101.16 (2008): 166601.

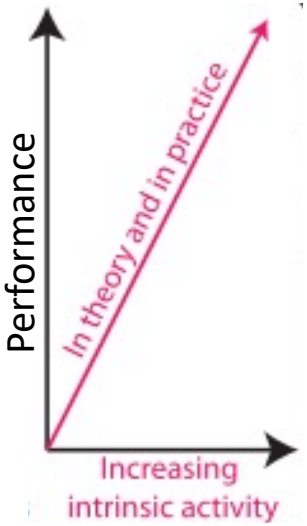

Intercalation

Confinement

Alloy

Adsorbates

Core-shell

Polymorph

…

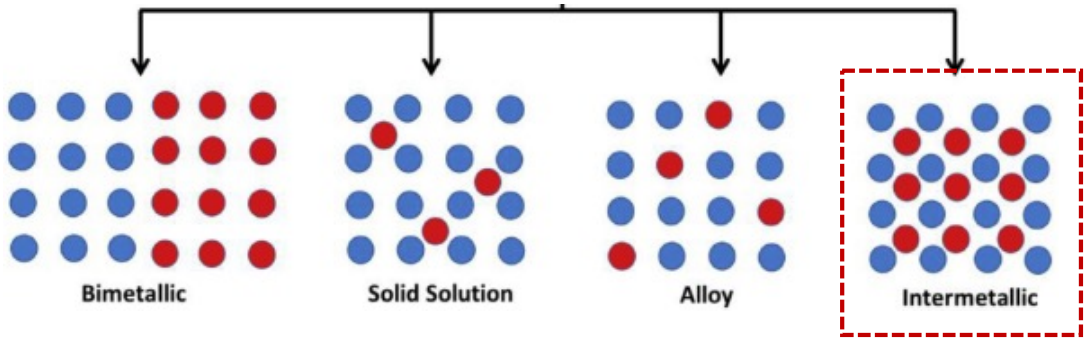

- Geometric arrangement
- Fixed atomic position
- Homogeneous distribution

[1] Seh, Zhi Wei, et al. *Science* 355.6321 (2017): eaad4998;

Brewer Intermetallic compound

Brewer intermetallic compounds [1]*Materials chemistry and physics*, *22*(1989), 1-26.

Hypo-d-electronic components: Hf, Zr, Nb, Ti, V, Mo, Cr, W

Hyper-d-electronic components: Co , Ni, Pt, Pd, Fe, Ir

Strong hypo–hyper-d-electronic interaction:

Adaptable M-H bond/ enhanced hydrogen evolution.

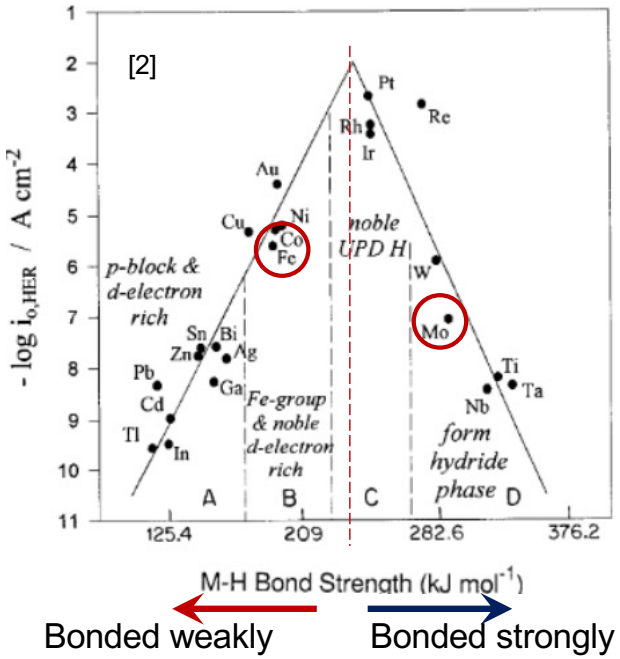

Co_3Mo particles@np-Cu

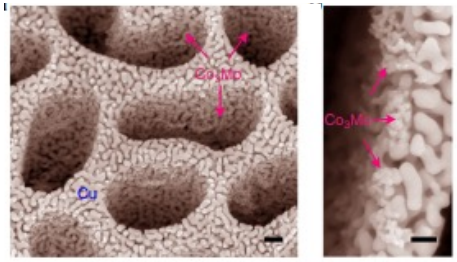

[3]*Nature communications* 11.1 (2020): 1-10.

Co_3Mo/Co_7Mo_6 particles

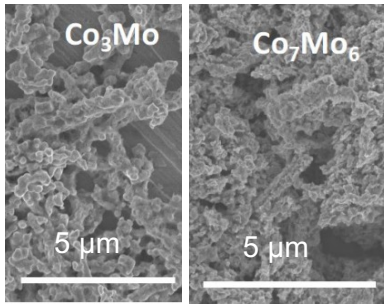

[4] *Hydrogen*, *1*(1), 11-21.

$MoNi_4/MoO_2$@Ni

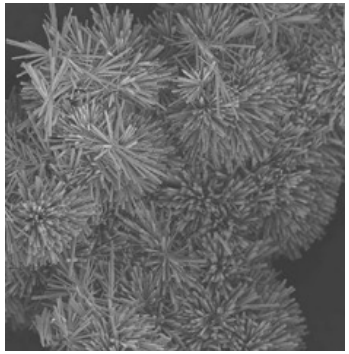

[5] *Nature communications*, *8*(1), 1-8

[2] *Electrochimica Acta*, *45*(25-26), 4075-4083.

Morphology evolution in liquid metal dealloying

Nanoporous μ-Co_7Mo_6 after LMD at 973 K for 120s

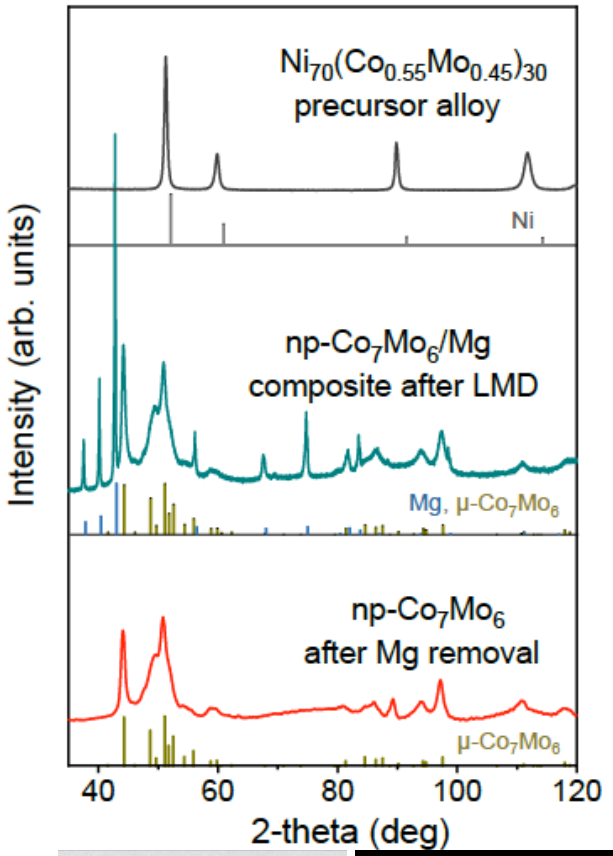

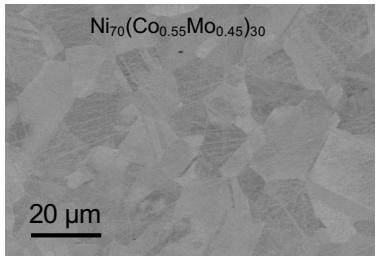

FCC precursor alloy with grain size of ~15 μm

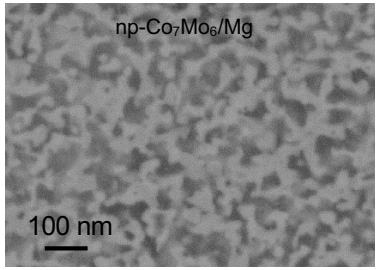

μ-Co_7Mo_6 with solidified Mg phase

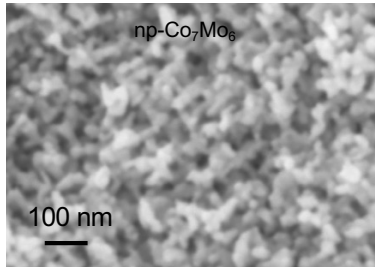

Free-standing np-Co_7Mo_6 in ~30 nm

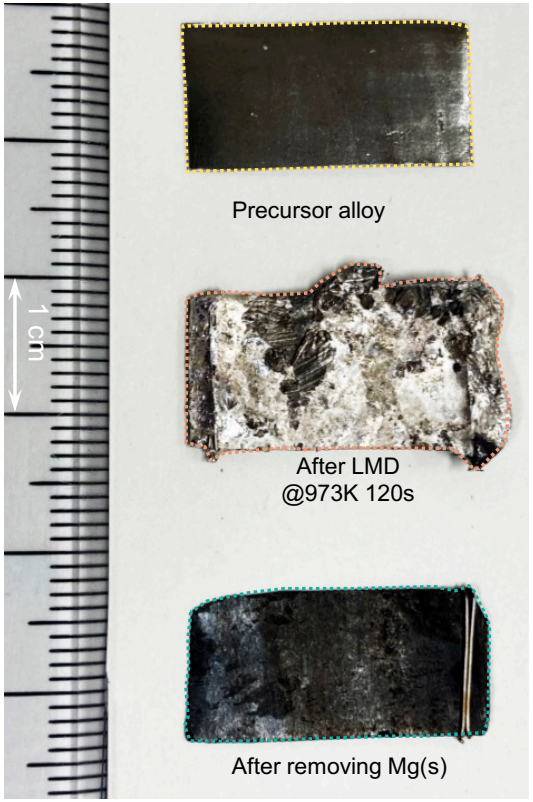

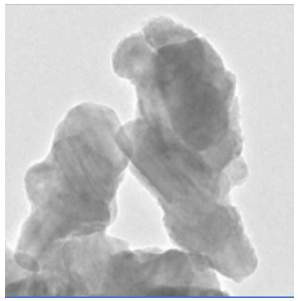

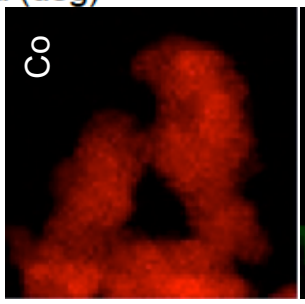

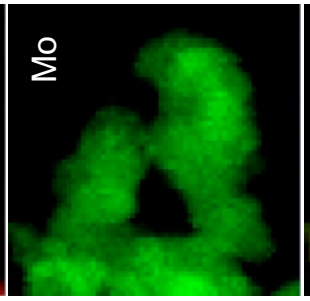

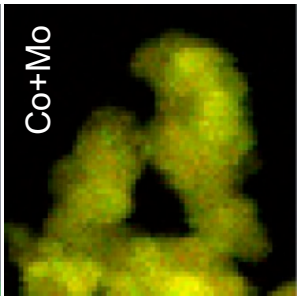

Uniform distribution of Co and Mo in the ligaments

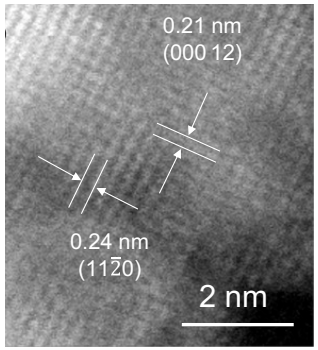

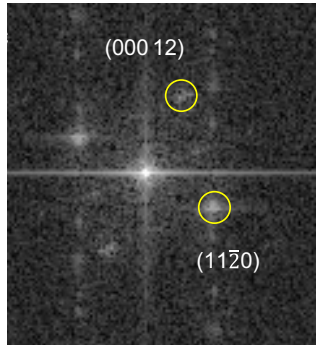

Song, Ruirui, et al. *Nature communications* 13.1 (2022): 1-12.

Porous Mo, Fe, $Cr_{50}Mo_{50}$, μ-Co_7Mo_6 and μ-Fe_7Mo_6

LMD performed at 973 K 120 s with $Ni_{70}(Mo_xM_y)_{30}$ alloy

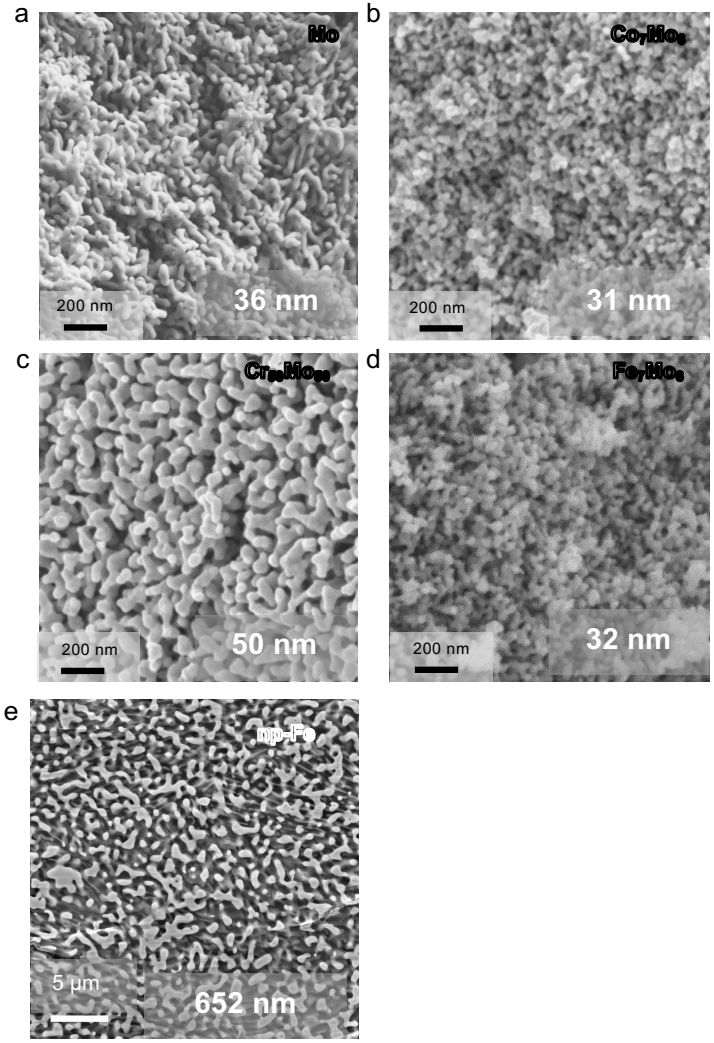

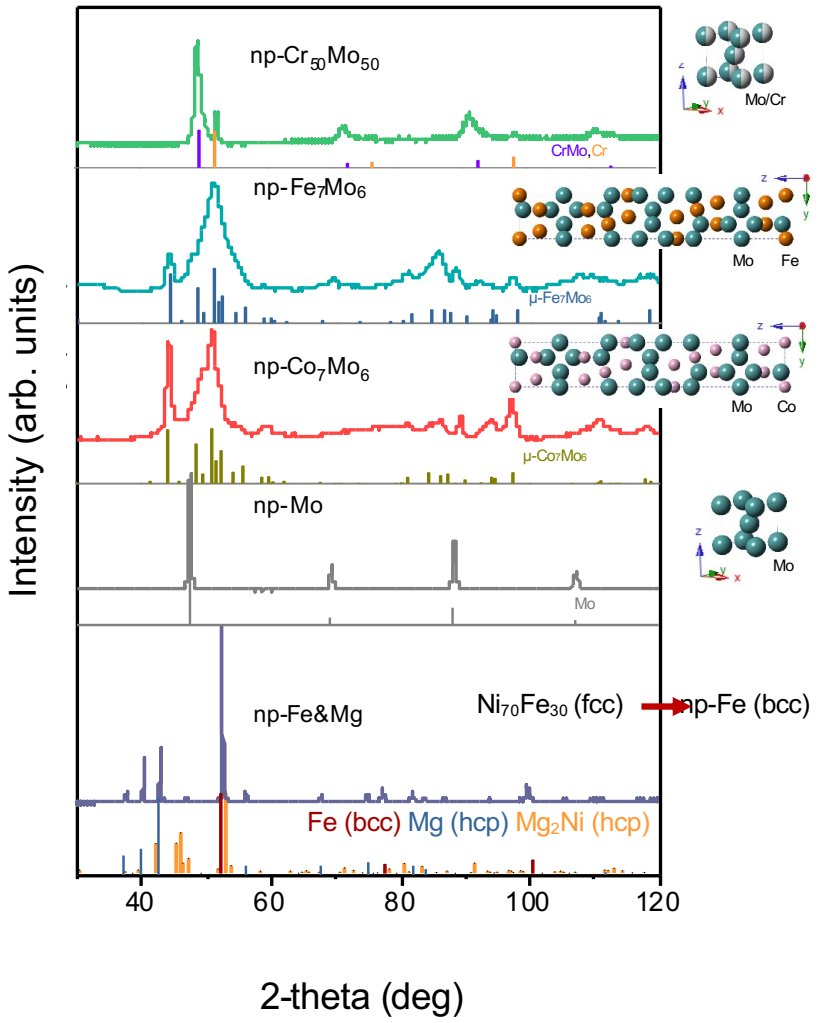

- The ligament sizes varied on the remained composition.
- The phases of ligament were obtained as designed.

Song, Ruirui, et al. *Nature communications* 13.1 (2022): 1-12.

Ligament size scaled with homologous temperature

$$E_a = KT_m$$

E_a : Activation energy of diffusion T_m : Melting temperature K :Constant

Diffusion in Solids-Fundamentals, Methods, Materials, Diffusion-Controlled Processes

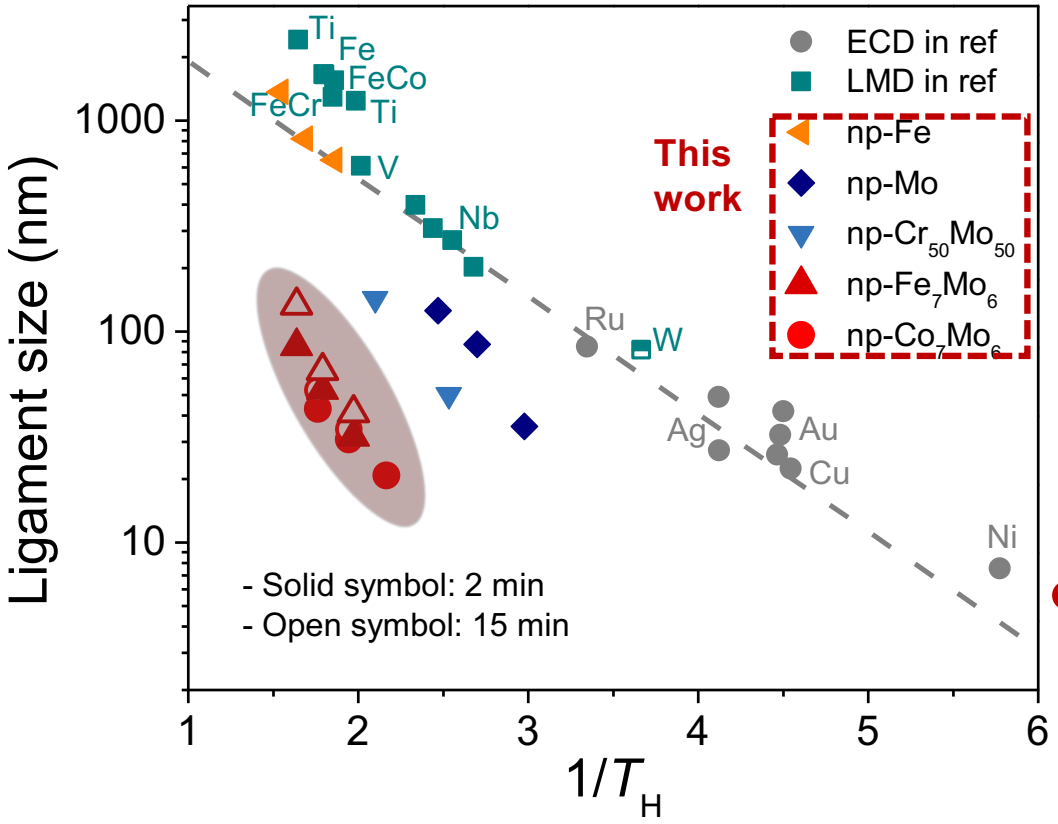

$$d(t)^n = D_0 t \exp\left(\frac{-E}{RT}\right) \quad T_H = T_{dealloy}/T_m$$

$$\log(d) = K'(1/T_H) + K''$$

T_H : Homologous temperature,

T_m: Melting point of the ligament components,

$T_{dealloy}$: Dealloying temperature.

K' and K'' : Constant.

- A surface-diffusion-controlled ligament size varied on homologous temperature.

- A distinct deviation from the conventional scaling relation is observed for nanoporous μ-Co_7Mo_6 and μ-Fe_7Mo_6.

Song, Ruirui, et al. *Nature communications* 13.1 (2022): 1-12.

Diffusivities calculated by molecular dynamics simulations

Calculated by Masayuki Okugawa Sensei, Osaka University

900 K–1200 K for 200 ps with zero external pressure (*NPT*), with molten Mg.

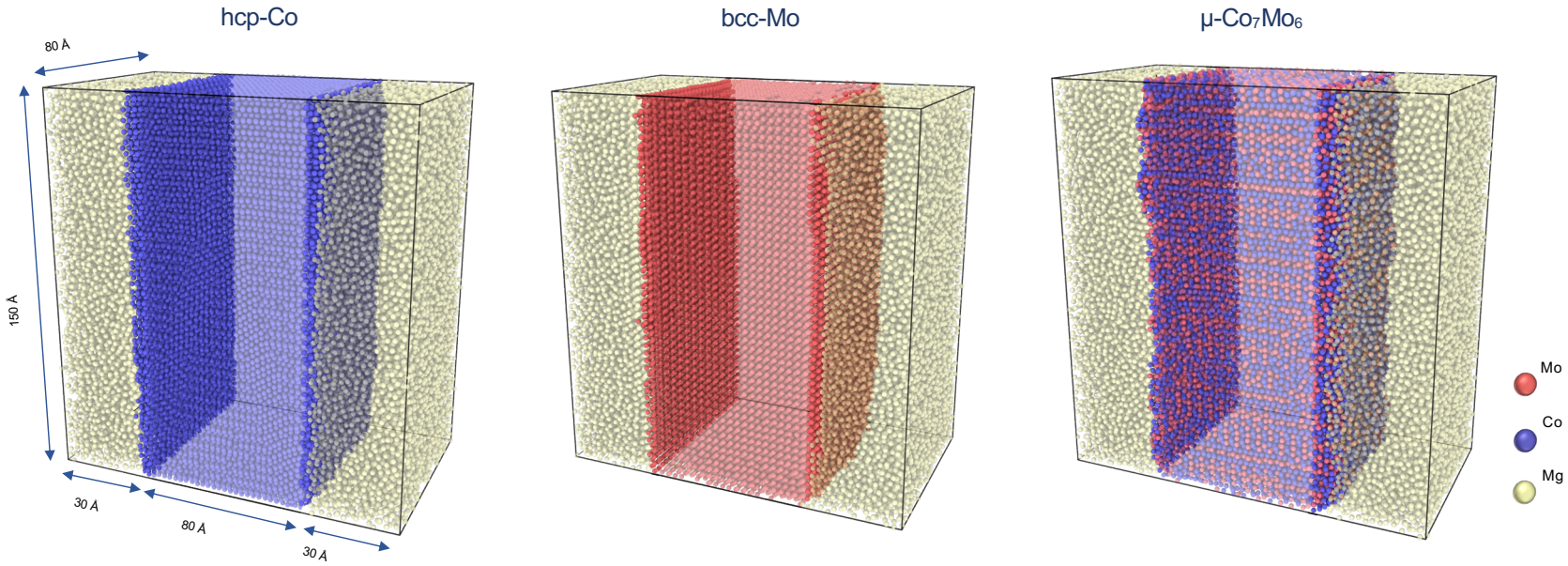

14 nm × 15 nm × 8 nm model

Einstein relation combined with mean square displacement (MSD)

$$D = \frac{\langle R^2 \rangle}{6\tau}.$$

R: The total displacement composed of many individual displacements r_i.

τ: the time for displacement, τ =t-t_0.

Song, Ruirui, et al. *Nature communications* 13.1 (2022): 1-12.

Diffusivities calculated by molecular dynamics simulations

Calculated by Masayuki Okugawa Sensei, Osaka University

The obtained average diffusivities were plotted against $1/T_H$.

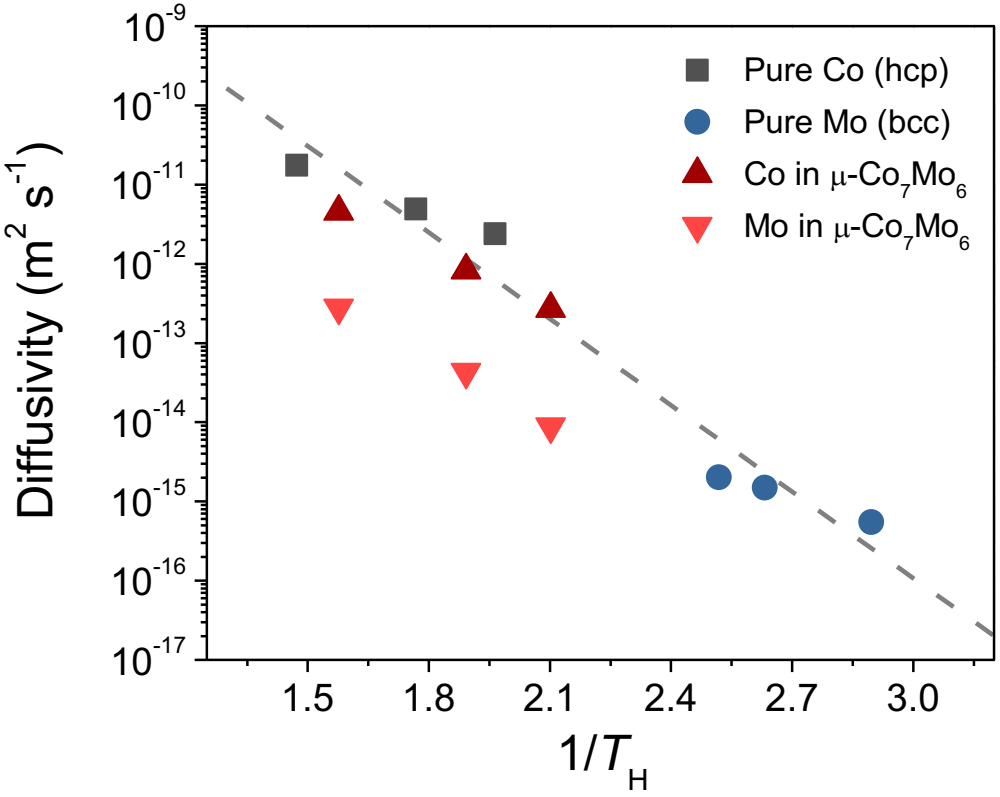

- Diffusivities of Co and Mo in ordered μ-Co_7Mo_6 are **impeded** compared with the Co-hcp and bcc-Mo.
- The intermetallic phase provides **a large energy barrier** for the diffusion of Co and Mo atoms.

Diffuse atom	hcp-Co	bcc-Mo	Co in μ-Co_7Mo_6	Mo in μ-Co_7Mo_6
Activation energy (kJ mol^{-1})	59.8	84.2	**84.7**	**102.5**

Song, Ruirui, et al. *Nature communications* 13.1 (2022): 1-12.

Evolution of ultrafine nanoporous intermetallic compounds

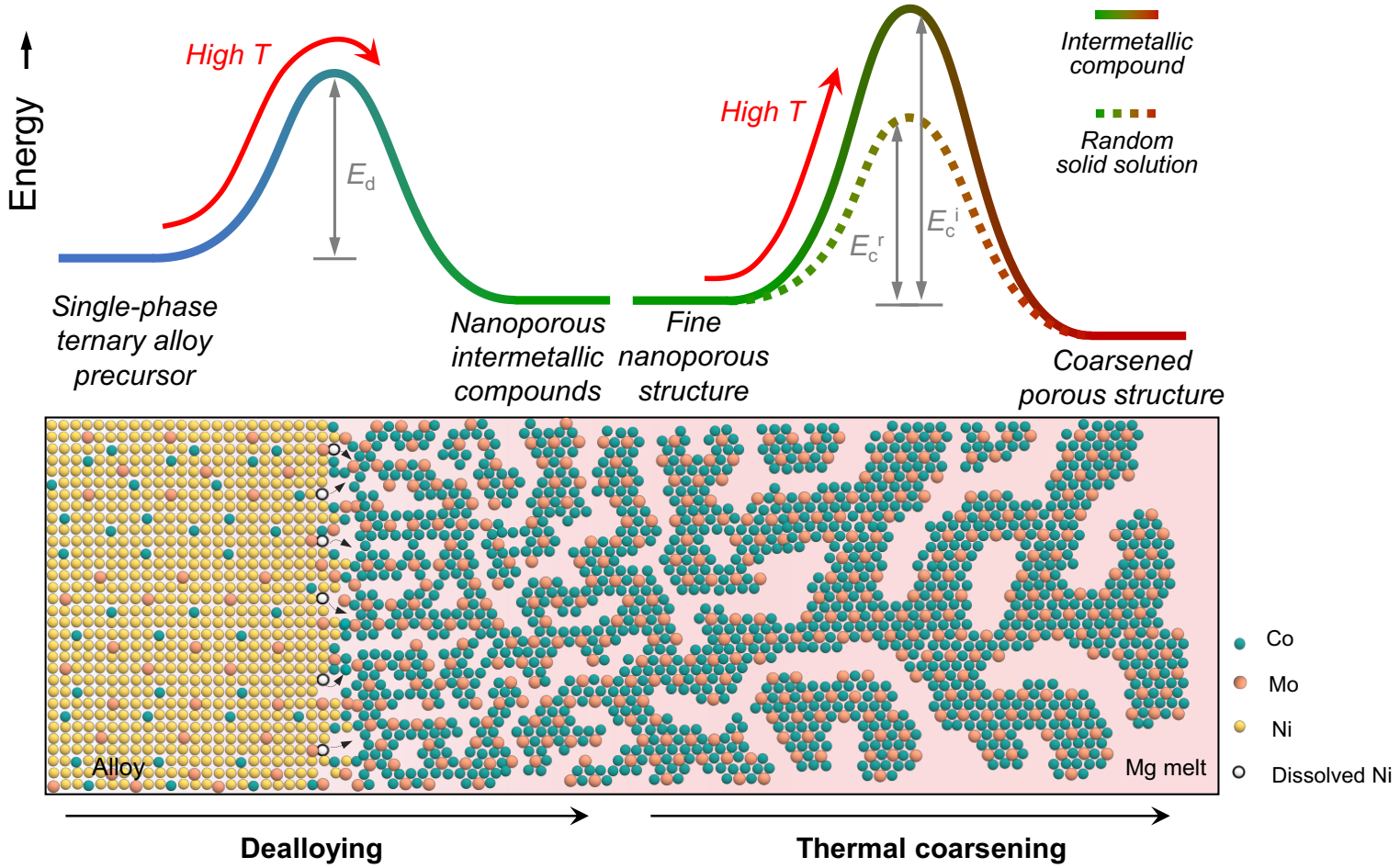

- High temperature in LMD overcome the barrier of selectively dissolving of Ni;
- Concurrent formation of μ-Co_7Mo_6 self-assembly evolved into bicontinuous porous structure;
- Large kinetic barrier for surface diffusion in μ-Co_7Mo_6 impeded further coarsening.

Song, Ruirui, et al. *Nature communications* 13.1 (2022): 1-12.

Electrocatalytic performance in hydrogen production

Cooperated with Assist. Prof. Jiuhui Han from FRIS, Tohoku Univ. and Prof. Mingwei Chen from The Johns Hopkins Univ.

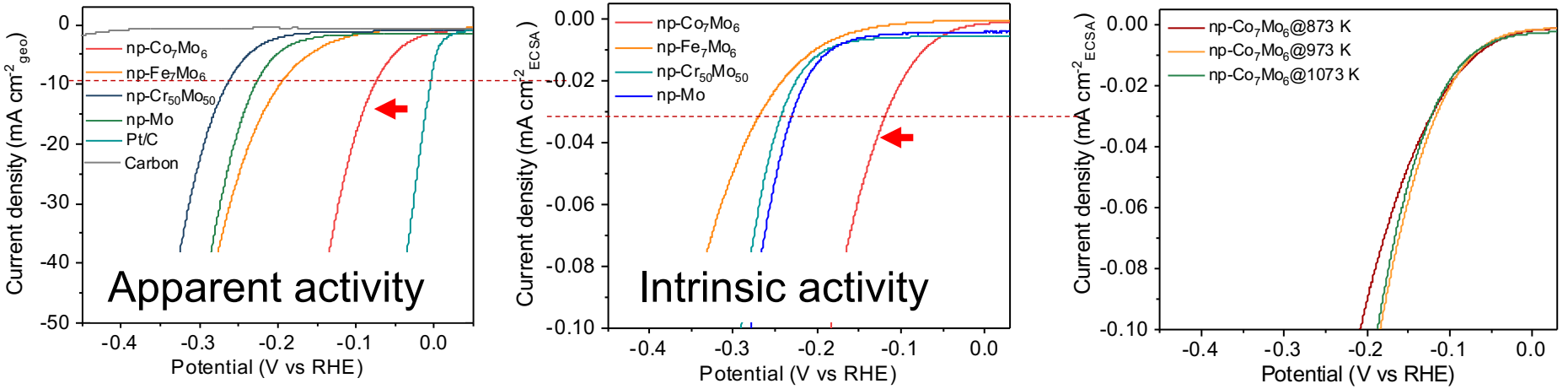

- Balancing the intrinsic reaction kinetics and accessibility of active sites.

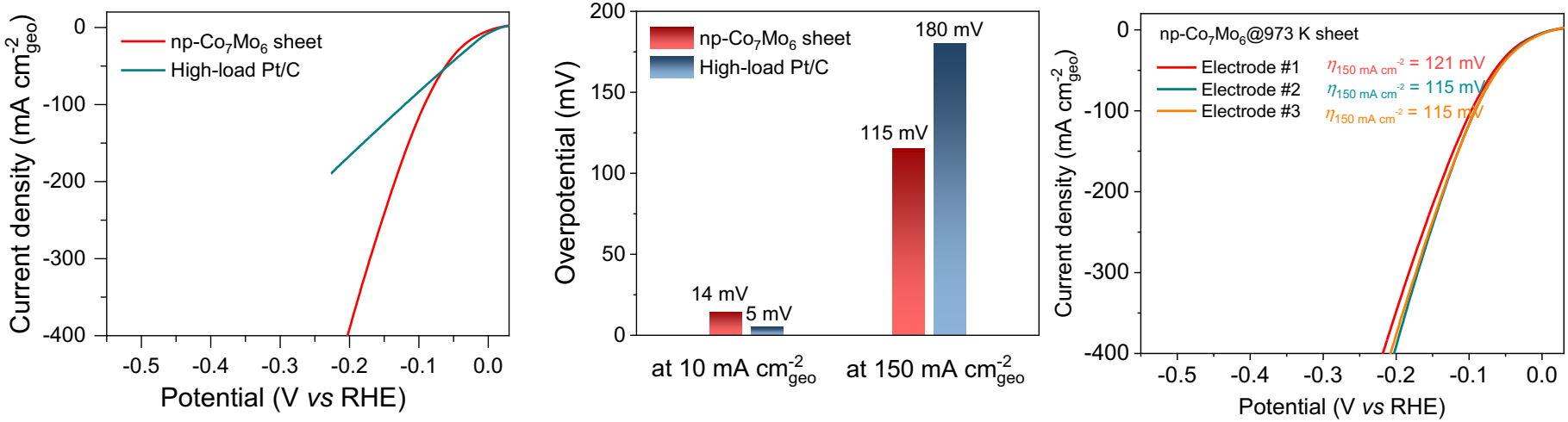

- Low-current-density property : **intrinsic activity**.
- Higher current densities : **ion and gas transport on active sites**.
- The 3D bicontinuous pore: **enhancing mass transport**.

Song, Ruirui, et al. *Nature communications* 13.1 (2022): 1-12.

Durability of self-supported np-Co_7Mo_6 electrocatalyst

Cooperated with Assist. Prof. Jiuhui Han from FRIS, Tohoku Univ. and Prof. Mingwei Chen from The Johns Hopkins Univ.

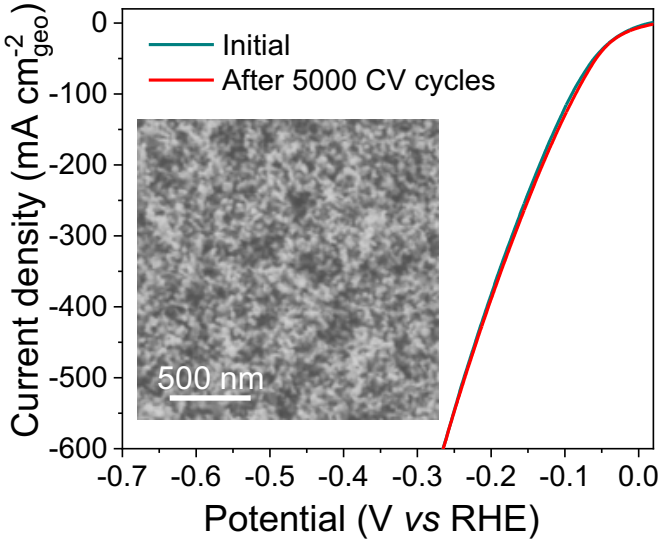

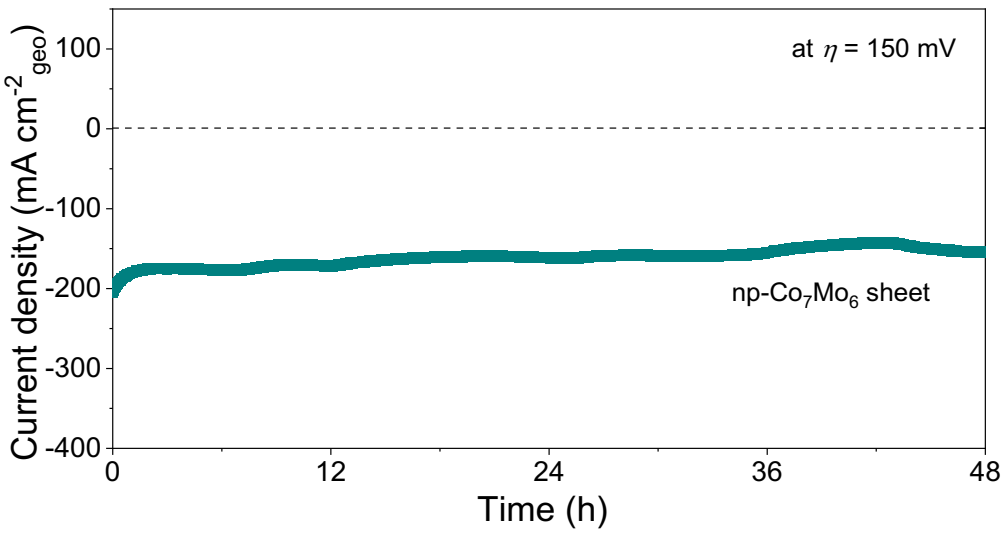

- A negligible shift in the HER polarization curves after 5000 cycles
- There is no apparent current decay over the long-term test for 48 h.

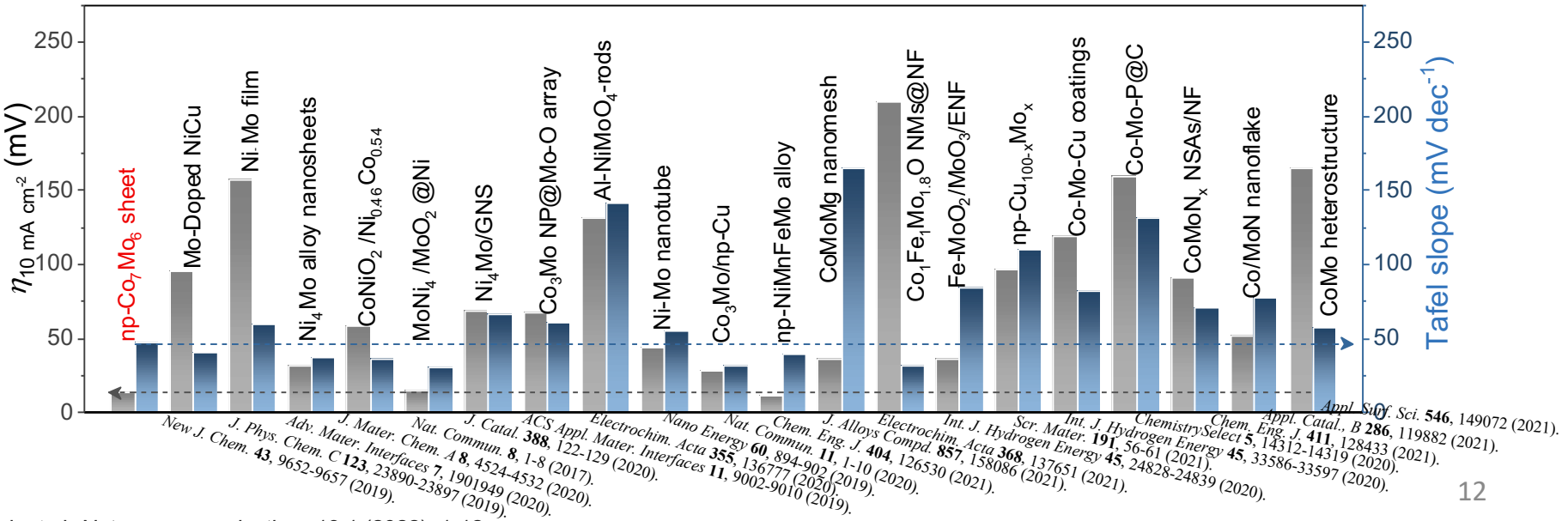

New J. Chem. **43**, 9652-9657 (2019).
J. Phys. Chem. C **123**, 23890-23897 (2019).
Adv. Mater. Interfaces **7**, 1901949 (2020).
J. Mater. Chem. A **8**, 4524-4532 (2020).
Nat. Commun. **8**, 1-8 (2017).
J. Catal. **388**, 122-129 (2020).
ACS Appl. Mater. Interfaces **11**, 9002-9010 (2019).
Electrochim. Acta **355**, 136777 (2020).
Nano Energy **60**, 894-902 (2019).
Nat. Commun. **11**, 1-10 (2020).
Chem. Eng. J. **404**, 126530 (2021).
J. Alloys Compd. **857**, 158086 (2021).
Electrochim. Acta **368**, 137651 (2021).
Int. J. Hydrogen Energy **45**, 24828-24839 (2020).
Scr. Mater. **191**, 56-61 (2021).
Int. J. Hydrogen Energy **45**, 33586-33597 (2020).
ChemistrySelect **5**, 14312-14319 (2020).
Chem. Eng. J. **411**, 128433 (2021).
Appl. Catal., B **286**, 119882 (2021).
Appl. Surf. Sci. **546**, 149072 (2021).

Song, Ruirui, et al. *Nature communications* 13.1 (2022): 1-12.

Conclusions

Fabrication of nanoporous Mo-based intermetallic compound

- Porous μ-Co_7Mo_6 sized in ~30.8 nm was obtained at 973 K for 120s.

Application for hydrogen evolution reaction catalyst

- Nanoporous μ-Co_7Mo_6 can balance the intrinsic activity and mass transport at high current densities.
- Self-supported nanoporous μ-Co_7Mo_6 is among the best performances reported for non-precious Mo-based HER electrocatalysts thus far.

Supported by Japan Society for the Promotion of Science (JSPS) KAKENHI (Grant Nos. 21J12719, Ruirui Song)

Next

- Research on the mechanism of reaction front coupled with intermetallic phase forming in LMD.
- Developing nanoporous intermetallic compounds electrocatalysts for other electrochemical reaction.